

Laboratory measurements of flow through wellbore cement-casing microannuli

Stormont, J.C., Ahmad, R., Ellison, J. and Taha, M.R.

Department of Civil Engineering, University of New Mexico, Albuquerque, NM, USA

Matteo, E.N.

Sandia National Laboratories, Albuquerque, NM, USA.

Copyright 2015 ARMA, American Rock Mechanics Association

This paper was prepared for presentation at the 49th US Rock Mechanics / Geomechanics Symposium held in San Francisco, CA, USA, 28 June-1 July 2015.

This paper was selected for presentation at the symposium by an ARMA Technical Program Committee based on a technical and critical review of the paper by a minimum of two technical reviewers. The material, as presented, does not necessarily reflect any position of ARMA, its officers, or members. Electronic reproduction, distribution, or storage of any part of this paper for commercial purposes without the written consent of ARMA is prohibited. Permission to reproduce in print is restricted to an abstract of not more than 200 words; illustrations may not be copied. The abstract must contain conspicuous acknowledgement of where and by whom the paper was presented.

ABSTRACT: Microannuli that develop along the cement-casing interface have been identified as common leakage pathways in wellbores. We have developed an experimental system that allows laboratory testing of wellbore specimens which are comprised of a cement sheath cast on a steel casing. Specimens were produced with a range of flaws including microannuli between the steel casing and the cement. The system allows independent application of confining pressures to 35 MPa and internal (casing) pressures to 20 MPa while gas flow is measured through the specimens along the wellbore axis. We present the gas flow results in terms of the hydraulic aperture of microannuli as a function of confining pressure and internal pressure. The interpreted hydraulic apertures vary depending on how the microannuli were created. The hydraulic apertures are sensitive to stress changes, and decrease non-linearly with increasing stress across the microannuli in a manner similar to fractures in rocks and other materials.

1. INTRODUCTION

The integrity of wellbore systems - consisting of casing, cement sheath and adjacent rock formation – is of critical importance to many sub-surface operations including CO₂ sequestration, oil and gas exploration and production, and geothermal energy development. Wellbore systems often have a significant vertical permeability due to the presence of flaws (factures, voids) that allow for fluid migration along the axis of the wellbore [e.g., 1]. The cement-casing interface, herein referred to as the microannulus, has been identified as a common leakage pathway [2, 3, 4]. The flaws are created by a range of factors during well cementing and subsequent well operations, including incomplete drilling mud removal prior to cementing, cement shrinkage, and changes in pressures and temperatures within the casing [5].

The microannulus is a discrete fracture-like flaw along the cement-casing interface, and its permeability is expected to be a function of stresses that would tend to open or close it. These stresses include internal pressures in the casing as well as the external or confining stresses acting on the wellbore system. The external stresses that acts on the cement sheath are a function of many factors, including the overburden pressure, the tendency of the rock to creep, deformations

in the overburden and wellbore systems due to reservoir compaction or expansion, changes in formation pore pressure, expansion/contraction of the cement, and pressures and temperatures in the casing [6, 7]. The pressure within a casing can also vary, depending on the condition and use of the wellbore. In an abandoned well, the casing pressure will depend on what material (water, mud, cement), if any, remains in the casing. While in operation, an injection well will have a casing pressure in excess of the formation pore pressure, but less than the overburden pressure to prevent formation failure. Casing pressures are particularly important for the condition of the cement-casing interface as the contact stress across the interface depends in part on the casing pressure. Temperature changes in the casing fluids can also induce casing expansion and contraction, imposing stresses on the cement-casing interface.

An understanding of microannulus flow as a function of stress conditions is useful for a number of applications. Estimates of flow through a leaky wellbore with a microannulus will be improved if the stress conditions that are possible for a particular well are accounted for. The impact of well operations on wellbore integrity would be better understood and perhaps managed if the microannulus response to stress was understood. This knowledge would also inform efforts to repair leaky wellbores which often involve attempts to “squeeze”

repair materials into the microannulus. In this paper, we report on laboratory measurements of flow through microannuli under varying confining pressures and internal casing pressures to provide insight how microannuli respond to a range of stress conditions.

2. EXPERIMENTAL SYSTEM

The experimental configuration is shown in Figure 1. Specimens, consisting of a cement sheath cast on a steel casing with microannuli, are subjected to confining pressures and casing pressures in a pressure vessel that allows simultaneous measurement of gas flow along the axis of the specimen.

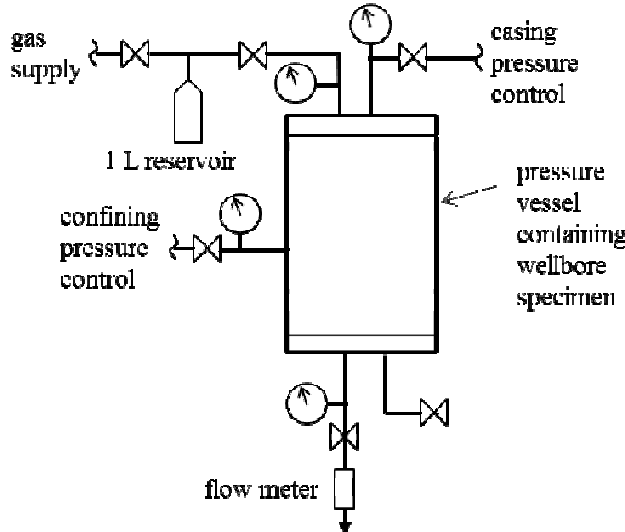


Figure 1 – Schematic of experimental configuration used to measure gas flow through cement-casing specimens under variable confining pressure and casing pressure.

Test specimens were cast in a mold that included a central steel pipe (Figure 2). Class G cement was used (water/cement ratio of 0.3). The finished specimens have an outer diameter of 96 mm, a casing inner diameter of 52.9 mm, and a length of 200 mm. The casing thickness varied from 1.5 to 3.2 mm between different specimens. The specimens were cured at 55 °C in a humid environment for a minimum of 14 days prior to testing.



Figure 2 – Specimen with cement sheath cast around a steel casing.

“Large microannuli” were created by wrapping the casing in release film prior to casting the specimen. After 24 hours, the release film and casing was removed. The casing was then reinserted into cement sheath and the specimen was allowed to cure. After curing, the casing was loose enough to be slid in and out of the cement sheath. “Small microannuli” were created by cooling the interior of the casing of a cured specimen with liquid nitrogen or dry ice. In response to the cooling, the casing contracted sufficiently to de-bond with the cement. Once the temperature returned to ambient, the casing remained tight in the cement sheath. In some instances, an axial force was applied to the casing to ensure it was de-bonded.

The pressure vessel (Figure 3) allows independent application of confining pressure to 30 MPa and internal (casing) pressure to 20 MPa. The end pieces of the vessel include a steel boss that fits into the casing to isolate it. The end pieces also include ports that access the ends of the specimen for flow testing.

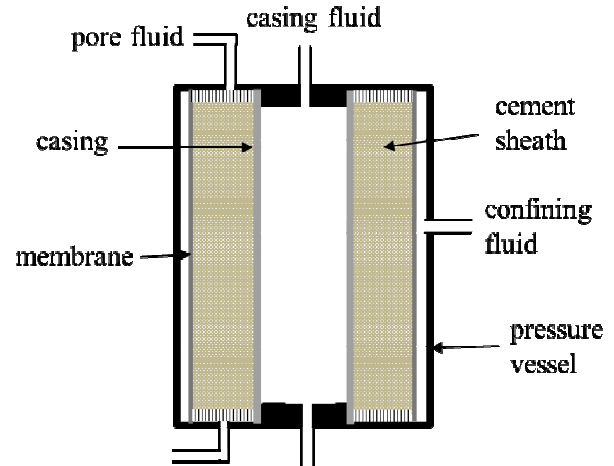


Figure 3 – Schematic of cross-section of pressure vessel for testing cement-casing specimens.

The permeameter connects to the upstream and downstream ports on the pressure vessel. The permeameter system can accommodate gas pressures to 15 MPa, and allows for both steady state and transient measurements to be made. Steady-state flow rates in the range of 0.1 to 10 L/min are made with a flow meter. Steady-state flow rates between 0.001 L/min and about 0.1 L/min are made by monitoring the rate of pressure change in a 1 L reservoir. Steady-state measurements can be made with a backpressure greater than atmosphere. For lower flow rates, transient measurements are made using pulse decay methods.

3. DATA ANALYSES

The measured flowrates through the specimens with flaws were interpreted using the Forchheimer equation [8] which includes both viscous (Darcy) and inertial (non-linear) flow terms,

$$-\nabla P = \frac{\mu}{kA} Q + \frac{\beta \rho}{A^2} Q^2 \quad (1)$$

where ∇P is the gradient, Q is the volumetric flowrate, k is the permeability, β is the inertial coefficient, A is the cross sectional area involved in the flow, μ is viscosity, and ρ is density. Eqn (1) can be rewritten as

$$-\frac{\nabla P}{Q} = \frac{\mu}{kA} + \frac{\beta \rho}{A^2} Q \quad (2)$$

Plotting the left side of (2) vs. the flowrate yields a straight line with a slope that is a function of the inertial coefficient and an intercept proportional to permeability. In the absence of non-linear flow, the slope will be zero.

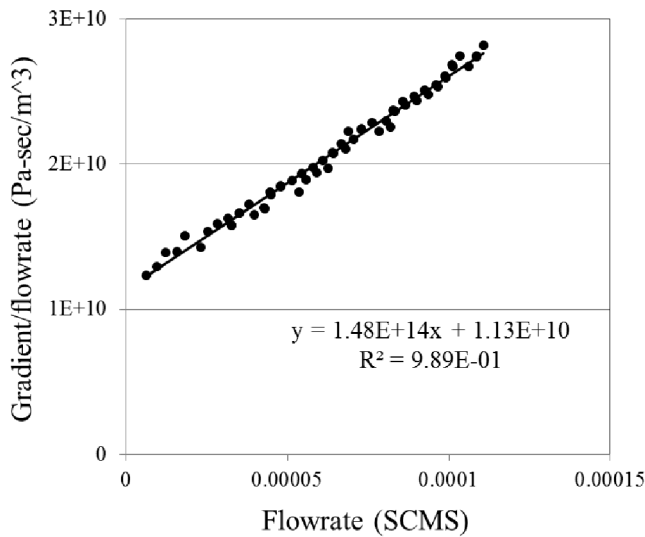


Figure 4 – Experimental data plotted to determine permeability from tests that include non-linear flow.

The specimens with flaws yielded flow rates that were more than 3 orders of magnitude greater than that for intact specimens (i.e., cement) under comparable conditions. Flow was therefore assumed to occur only through the flaws, and the calculated permeability was interpreted as a hydraulic aperture (h) using the so-called cubic law [9]

$$h^3 = \frac{12kA}{w} \quad (3)$$

where w is the flaw width which for these tests is the outer circumference of the casing.

Gas slip effects were evaluated from data collected at different mean gas pressures [10] and from data collected with different gases [11]. In the tests reported here, the flow paths were sufficiently large that gas slip effects were not observed.

4. RESULTS

4.1. Flow through large microannuli

Hydraulic aperture as a function of confining pressure for a specimen with a large microannulus is shown in Figure 5. The arrows on the figure indicate the loading path taken between measurements. The initial hydraulic aperture was 100 microns at a confining pressure of 4 MPa. With increasing confining pressure, the hydraulic aperture decreases. After about 20 MPa, the rate of decrease of the hydraulic aperture with confining pressure decreases. As the confining pressure is reduced from 35 MPa to 20 MPa, the hydraulic apertures are close to those measured on the loading path. At the final confining pressure of 14 MPa, the hydraulic aperture is smaller than that it was at the same confining pressure on the initial loading path.

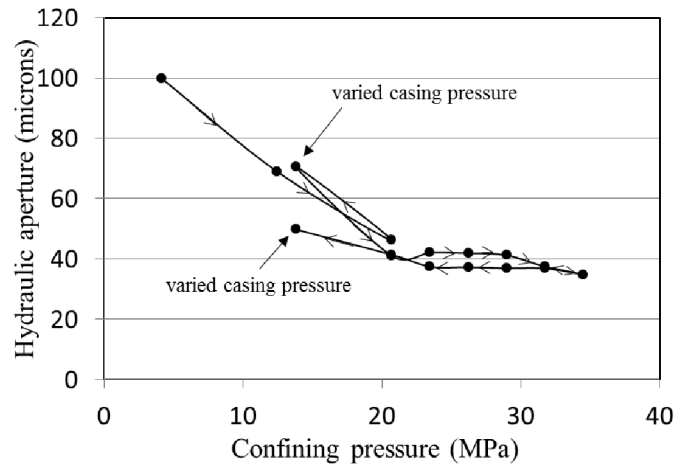


Figure 5 – Hydraulic aperture vs. confining pressure for specimen with large microannulus.

At 14 MPa on the loading and unloading path, the internal casing pressure was varied from 0 to 14 MPa. The change in hydraulic aperture in response to the change in casing pressure is shown in Figure 6. Compared to changes in confining pressure, the hydraulic aperture is much less sensitive to changes in casing pressure largely because of the relative stiffness of the steel compared to that of the cement. An alternative way to present these results is in terms of the elastic contact stress, which is the radial stress at the cement-casing interface calculated from an elastic solution for a bi-material hollow cylinder [12]. The contact stress was calculated for the geometry and material properties for this specimen as a function of the applied confining and internal casing pressures. When the hydraulic aperture results are given in this form, they reveal that the casing pressure changes produce relatively small changes in the calculated elastic stress across the cement-casing interface compared to those produced from casing pressure changes. While generally insightful, the elastic solution is limited: even when results are presented in terms of elastic contact

stress, the rate of change of the hydraulic aperture in response to casing pressure is less than that for confining pressure.

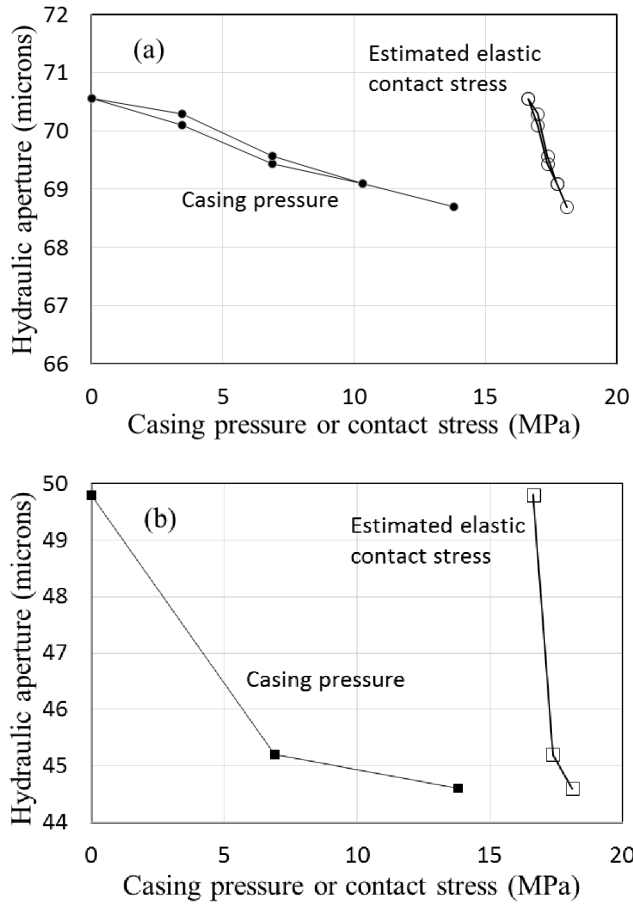


Figure 6 – Hydraulic aperture as a function of casing pressure (solid symbols) and calculated elastic contact stress (open symbols) for test conducted at confining pressure at 14 MPa during (a) initial loading, and (b) unloading path.

When this specimen was removed from the pressure vessel, the casing could still be easily removed and replaced. The specimen was placed back in the pressure vessel and retested. These results are shown in Figure 7 with the dashed line, and the initial test results are shown with the solid line. The initial hydraulic aperture was somewhat larger than during the initial test. With increasing confining pressure and during unloading, the hydraulic apertures are similar to those from the initial testing.

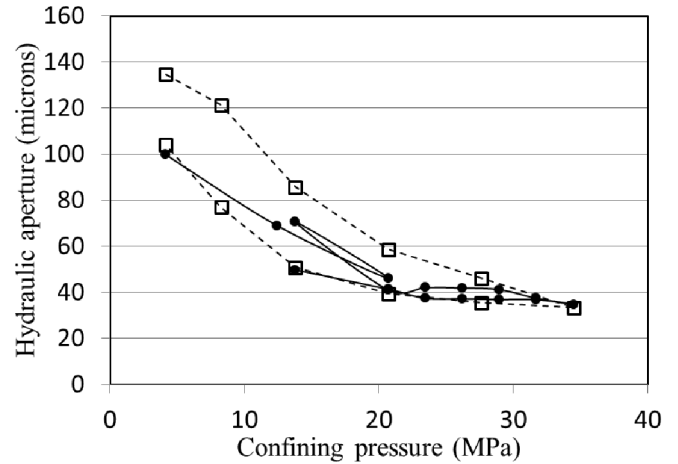


Figure 7 - Hydraulic aperture vs. confining pressure for specimen with large microannulus that was retested (dashed line). Initial test results are shown with solid line.

4.2. Flow through small microannuli

Hydraulic aperture as a function of confining pressure for specimens with small microannuli is shown in Figure 8. The arrows denote the loading path. With increasing confining pressure, the hydraulic aperture decreases. Upon unloading, the hydraulic aperture increases only slightly and is smaller than that on the loading path. These hydraulic apertures are about one order of magnitude smaller than that for the specimens with a large microannulus.

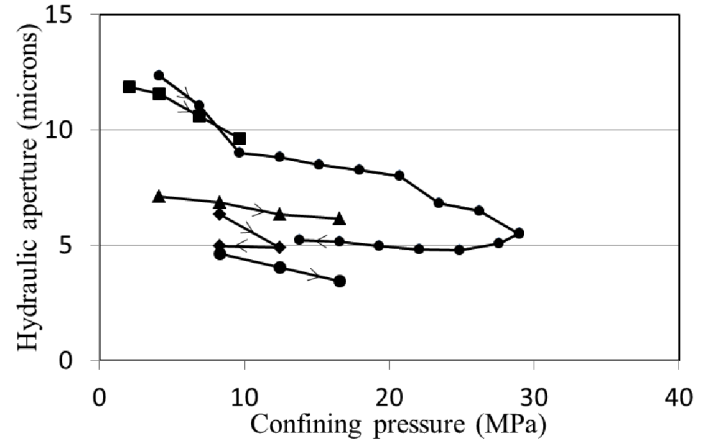


Figure 8 – Hydraulic aperture vs. confining pressure for specimens with small microannuli.

Another specimen with a small microannulus was subjected to changes in casing pressure at different two values of confining pressure. The results are given in Figure 9 in terms of the elastic circumferential stress, which is the circumferential stress in the cement adjacent to the cement – casing interface calculated using the bi-material hollow cylinder elastic solution [12]. For the tests at both confining pressures, the casing pressure was increased above the confining pressure. The increase in hydraulic aperture for the specimen tested at a confining

pressure of 4.1 MPa coincides with the calculated elastic circumferential stress becoming negative, suggesting that the cement may have failed in tension. A fracture in the cement was observed upon removing the specimen from the pressure vessel.

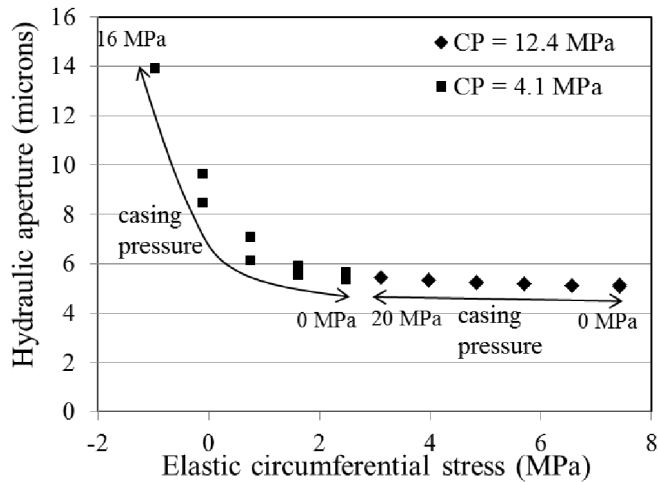


Figure 9 – Hydraulic aperture as a function of calculated elastic circumferential stress. Confining pressure was held constant and casing pressure varied during these tests.

5. DISCUSSION

Interpreted hydraulic apertures varied by about an order of magnitude depending on the type of microannulus. For the large microannuli, where the casing was loose in the cement sheath, initial apertures were 100 microns and larger. The minimum aperture for these specimens was 40 microns under confining pressures above about 20 to 30 MPa. In contrast, small microannuli, where the casing is tight in the cement but de-bonded, had initial hydraulic apertures around 10 microns that decreased by about half under large confining pressures. These results suggest that once a wellbore system experiences conditions sufficient to de-bond the cement from the casing, this location will remain a discrete flow path even under relatively large stresses that tend to close the microannulus.

The measurements indicate that the hydraulic apertures of the microannuli were found to respond to changes in confining stress and casing pressures. The non-linear decrease in hydraulic aperture with increasing stress across the interface is consistent with the typical response of fractures in rocks and cementitious materials. Because the permeability of the wellbore system is related to the cube of the hydraulic aperture, the potential flow through the wellbore system will change significantly depending on the stress state near the microannulus.

The elastic solution provides a useful first-order estimate of stresses in the vicinity of the cement-casing interface.

The calculated stress across the cement-casing contact accounts for the geometry and material properties of the wellbore system, and these stresses are generally consistent with the reduced sensitivity of the microannulus to changes in casing pressure compared to confining pressure. The elastic solution was also consistent with the development of tension in the cement from relatively large casing pressure. In order to link the measured changes in hydraulic aperture to the applied stress conditions, a wellbore model that incorporates stress-dependent stiffness of the microannulus is being developed.

ACKNOWLEDGEMENT

This material is based upon work supported by the U.S. Department of Energy (DOE) National Energy Technology Laboratory (NETL) under Grant Number DEFE0009562. This project is managed and administered by the DOE/NETL Storage Division and funded by DOE/NETL and cost-sharing partners. This paper was prepared as an account of work sponsored by an agency of the United States Government. Neither the United States Government nor any agency thereof, nor any of their employees, makes any warranty, express or implied, or assumes any legal liability or responsibility for the accuracy, completeness, or usefulness of any information, apparatus, product, or process disclosed, or represents that its use would not infringe privately owned rights. Reference herein to any specific commercial product, process, or service by trade name, trademark, manufacturer, or otherwise does not necessarily constitute or imply its endorsement, recommendation, or favoring by the United States Government or any agency thereof. The views and opinions of authors expressed herein do not necessarily state or reflect those of the United States Government or any agency thereof. Sandia National Laboratories is a multi-program laboratory managed and operated by Sandia Corporation, a wholly owned subsidiary of Lockheed Martin Corporation, for the U.S. Department of Energy's National Nuclear Security Administration under contract DE-AC04-94AL85000. SAND#

REFERENCES

- Watson, T.L., and S. Bachu. 2008. Identification of Wells With High CO₂-Leakage Potential in Mature Oil Fields Developed for CO₂-Enhanced Oil Recovery. *SPE 112924-MS*.
- Gasda, S. E., S. Bachu, and M. A. Celia. 2004. Spatial characterization of the location of potentially leaky wells penetrating a deep saline aquifer in a mature sedimentary basin. *Environ. Geol.*, 46(6–7), 707–720.
- Bachu, S. and D.B. Bennion. 2009. Experimental assessment of brine and/or CO₂ leakage through well cements at reservoir conditions. *Int. J. Greenhouse Gas Cont.*, 3, 494–501.
- Bellabara, M. 2008. Ensuring Zonal Isolation Beyond the Life of the Well. *Oilfield Review*, Spring, 8 – 31.

5. Zhang, M. and S. Bachu. 2011. Review of integrity of existing wells in relation to CO₂ geological storage: What do we know? *Int. J. Greenhouse Gas Cont.* 5, 826-840.
6. Hawkes, C.D., P.J. McLellan, and S. Bachu. 2005. Geomechanical Factors Affecting Geological Storage of CO₂ in Depleted Oil and Gas Reservoirs. *J. Can. Petr. Tech.* 44 (10), 2-61.
7. Orlic, B. 2008. Some Geomechanical Aspects of Geological CO₂ Sequestration. In Proceeding of the 12th International Conference of *International Association for Computer Methods and Advances in Geomechanics*, Goa, India, 1-6 October, 2204 – 2212.
8. Forchheimer, P., 1901, Wasserbewegung durch Boden, *Zeitz ver Deutch Ing.*, 45, 1782-1788.
9. Witherspoon, P.A., J. S. Wang,, K. Iwai, J.E.Gale. 1980, Validity of cubic law for fluid flow in a deformable rock fracture. *Water Res. Res.* 16 (6), 1016-1024.
10. Klinkenberg, L.J. 1941. The permeability of porous media to liquids and gases. *API Drill. Prod. Prac.* 200-213.
11. Stormont, J.C. and J. Daemen. 1992. An Alternative Method for Determining the Klinkenberg Correction, *ASTM Geotechnical Testing Journal*, 15, 409-413.
12. Ugwu, I. O. 2008. Cement fatigue and HPHT well integrity with application to life of well prediction. MS Thesis, Texas A&M University.